Antenna Theory: A Review

CONSTANTINE A. BALANIS, FELLOW, IEEE

Invited Paper

This paper is a tutorial on the theory of antennas, and it has been written as an introduction for the nonspecialist and as a review for the expert. The paper traces the history of antennas and some of the most basic radiating elements, demonstrates the fundamental principles of antenna radiation, reviews Maxwell's equations and electromagnetic boundary conditions, and outlines basic procedures and equations of radiation. Modeling of antenna source excitation is illustrated, and antenna parameters and figures-of-merit are reviewed. Finally, theorems, arraying principles, and advanced asymptotic methods for antenna analysis and design are summarized.

I. INTRODUCTION

For wireless communication systems, the antenna is one of the most critical components. A good design of the antenna can relax system requirements and improve overall system performance. A typical example is TV for which the overall broadcast reception can be improved by utilizing a high performance antenna. An antenna is the system component that is designed to radiate or receive electromagnetic waves. In other words, the antenna is the electromagnetic transducer which is used to convert, in the transmitting mode, guided waves within a transmission line to radiated free-space waves or to convert, in the receiving mode, free-space waves to guided waves. In a modern wireless system, the antenna must also act as a directional device to optimize or accentuate the transmitted or received energy in some directions while suppressing it in others [1]. The antenna serves to a communication system the same purpose that eyes and eyeglasses serve to a human.

The history of antennas [2] dates back to James Clerk Maxwell who unified the theories of electricity and magnetism, and eloquently represented their relations through a set of profound equations best known as *Maxwell's Equations.* His work was first published in 1873 [3]. He also showed that light was electromagnetic and that both light and electromagnetic waves travel by wave disturbances of the same speed. In 1886, Professor Heinrich Rudolph Hertz demonstrated the first wireless electromagnetic system. He was able to produce in his laboratory at a wavelength of 4 m a spark in the gap of a transmitting $\lambda/2$ dipole which was then detected as a spark in the gap of a nearby loop. It was not until 1901 that Guglielmo Marconi was able to send signals over large distances. He performed, in 1901, the first transatlantic transmission from Poldhu in Cornwall, England, to St. John's, Newfoundland.

His transmitting antenna consisted of 50 vertical wires in the form of a fan connected to ground through a spark transmitter. The wires were supported horizontally by a guyed wire between two 60-m wooden poles. The receiving antenna at St. John's was a 200-m wire pulled and supported by a kite. This was the dawn of the antenna era.

From Marconi's inception through the 1940's, antenna technology was primarily centered on wire related radiating elements and frequencies up to about UHF. It was not until World War II that modern antenna technology was launched and new elements (such as waveguide apertures, horns, reflectors, etc.) were primarily introduced. Much of this work is captured in the book by Silver [4]. A contributing factor to this new era was the invention of microwave sources (such as the klystron and magnetron) with frequencies of 1 GHz and above.

While World War II launched a new era in antennas, advances made in computer architecture and technology during the 1960's–1980's have had a major impact on the advance of modern antenna technology, and they are expected to have an even greater influence on antenna engineering in the 1990's and beyond. Beginning primarily in the early 1960's, numerical methods were introduced that allowed previously intractable complex antenna system configurations to be analyzed and designed very accurately. In addition, asymptotic methods for both low frequencies (e.g., Moment Method (MM), Finite-Difference, Finite-Element) and high frequencies (e.g., Geometrical and Physical Theories of Diffraction) were introduced, contributing significantly to the maturity of the antenna field. While in the past antenna design may have been considered a secondary issue in overall system design, today it plays a critical role. In fact, many system successes rely on the design and performance of the antenna. Also, while

Manuscript received November 26, 1990; revised March 1, 1991.

The author is with the Department of Electrical Engineering, Telecommunications Research Center, Arizona State University, Tempe, AZ 85287-7206.

IEEE Log Number 9105093.

in the first half of this century antenna technology may have been considered almost a "cut and try" operation, today it is truly an engineering art. Analysis and design methods are such that antenna system performance can be predicted with remarkable accuracy. In fact, many antenna designs proceed directly from the initial design stage to the prototype without intermediate testing. The level of confidence has increased tremendously.

The widespread interest in antennas is reflected by the large number of books written on the subject [5]. These have been classified under four categories: Fundamental, Handbooks, Measurements, and Specialized. In English, in all four categories, there were 4 books published in the 1940's, 9 in the 1950's, 17 in the 1960's, 20 in the 1970's, 69 in the 1980's, and 1 already in the 1990's. This is an outstanding collection of books, and it reflects the popularity of the antenna subject, especially since the 1950's. Because of space limitations, only a partial list is included here [1], [4], [6]–[32]. Some of these books are now out of print.

In this paper, the basic theory of antenna analysis, the parameters and figures-of-merit used to characterize antenna performance, and significant advances made in the last three decades that have contributed to the maturity of the field will be outlined. It will be concluded with a discussion of challenging opportunities for the future. Some of the material in this paper has been borrowed from the author's textbooks on antennas [1] and advanced electromagnetics [33].

II. Antenna Elements

Prior to World War II most antenna elements were of the wire type (long wires, dipoles, helices, rhombuses, fans, etc.), and they were used either as single elements or in arrays. During and after World War II, many other radiators, some of which may have been known for some time and others of which were relatively new, were put into service. This created a need for better understanding and optimization of their radiation characteristics. Many of these antennas were of the aperture type (such as open-ended waveguides, slots, horns, reflectors, lenses, and others), and they have been used for communication, radar, remote sensing, and deep space applications both on airborne and earth based platforms. Many of these operate in the microwave region. In this issue, reflector antennas are discussed in "The current state of the reflector antenna art—Entering the 1990's," by W. V. T. Rusch.

Prior to the 1950's, antennas with broadband pattern and impedance characteristics had bandwidths not much greater than about 2:1. In the 1950's, a breakthrough in antenna evolution was created which extended the maximum bandwidth to as great as 40:1 or more [34]–[36]. Because the geometries of these antennas are specified by angles instead of linear dimensions, they have ideally an infinite bandwidth. Therefore, they are referred to as *frequency independent*. These antennas are primarily used in the 10–10 000 MHz region in a variety of applications including TV, point-to-point communications, feeds for reflectors and lenses, and many others. This class of antennas is discussed in more detail in this issue in "Frequency-independent antennas and broad-band derivatives thereof," by P. E. Mayes.

It was not until almost 20 years later that a fundamental new radiating element, that has received a lot of attention and many applications since its inception, was introduced. This occurred in the early 1970's when the *microstrip* or *patch* antennas was reported [30], [37]–[44]. This element is simple, lightweight, inexpensive, low profile, and conformal to the surface. Microstrip antennas and arrays can be flush-mounted to metallic or other existing surfaces. Operational disadvantages of microstrip antennas include low efficiency, narrow bandwidth, and low power handling capabilities. These antennas are discussed in more detail in this issue in "Microstrip antennas," by D. M. Pozar. Major advances in millimeter wave antennas have been made in recent years, including integrated antennas where active and passive circuits are combined with the radiating elements in one compact unit (monolithic form). These antennas are discussed in this issue in "Millimeter wave antennas," by F. K. Schwering.

III. Theory

To analyze an antenna system, the sources of excitation are specified, and the objective is to find the electric and magnetic fields radiated by the elements. Once this is accomplished, a number of parameters and figures-of-merit that characterize the performance of the antenna system can be found. To design an antenna system, the characteristics of performance are specified, and the sources to satisfy the requirements are sought. In this paper, the analysis procedure is outlined. Synthesis procedures for pattern control of antenna arrays are discussed in this issue in "Basic array theory," by W. H. Kummer and "Array pattern control and synthesis," by R. C. Hansen. Theorems used in the solution of antenna problems are also discussed. Design and optimization procedures are presented in many of the other papers of this issue.

A. Radiation Mechanisms and Current Distribution

One of the most basic questions that may be asked concerning antennas is "how do they radiate?" A qualitative understanding of the radiation mechanism may be obtained by considering a pulse source attached to an open-ended conducting wire, which may be connected to ground through a discrete load at its open end. When the wire is initially energized, the charges (free electrons) in the wire are set in motion by the electric lines of force created by the source. When charges are accelerated in the source-end of the wire and decelerated (negative acceleration with respect to original motion) during reflection from its ends, it is suggested that radiated fields are produced at each end and along the remaining part of the wire [45]. The acceleration of the charges is accomplished by the external source in which forces set the charges in motion and produce the associated fields radiated. The deceleration of the charges at the end of the wire is accomplished by the internal (self) forces associated with the induced field due to the buildup of charge concentration at the ends of the wire. The internal forces receive energy from the charge buildup as its velocity is reduced to zero at the ends of the wire. Therefore, charge acceleration due to an exciting electric field and deceleration due to impedance discontinuities or smooth curves of the wire are mechanisms responsible for electromagnetic radiation. While both current density ($\boldsymbol{J}_i$) and charge density (q_{ve}) appear as source terms in Maxwell's equations (see (1b) and (1c)), charge is viewed as a more fundamental quantity. Even though this interpretation of radiation is primarily used for transient radiation, it can be used to explain steady-state radiation [45]. Another qualitative description of antenna radiation can be found in [1, ch. 1].

The previous explanation demonstrates the principles of radiation from a single wire. Let us now consider radiation and interference amplitude pattern (lobing) formation from a two-wire transmission line and antenna element, such as a linear dipole. We begin with the geometry of a lossless two-wire transmission line, as shown in Fig. 1(a). The movement of the charges creates a traveling wave current of magnitude $I_0/2$ along each of the wires. When the current arrives at the end of each of the wires, it undergoes a complete reflection (equal magnitude and 180° phase reversal). The reflected traveling wave, when combined with the incident traveling wave, forms in each wire a pure standing wave pattern of sinusoidal form as shown in Fig. 1(a). The current in each wire undergoes a 180° phase reversal between adjoining half periods. This is indicated in Fig. 1(a) by the reversal of the arrow direction.

For the two-wire balanced (symmetrical) transmission line, the current in a half-period of one wire is of the same magnitude but 180° out-of-phase from that in the corresponding half-period of the other wire. If, in addition, the spacing between the two wires is very small ($s \ll \lambda$), the fields radiated by the current of each wire are essentially canceled by those of the other. The net result is an almost ideal (and desired) nonradiating transmission line. As the section of the transmission line between $0 \leq \ell \leq \lambda/4$ begins to flare, as shown in Fig. 1(b), the current distribution is essentially unaltered in form in each of the wires. However, because the two wires of the flared section are not necessarily close to each other, the fields radiated by one do not necessarily cancel those of the other. Therefore, there is net radiation by the system.

Ultimately, the flared section of the transmission line can take the form shown in Fig. 1(c). This is the geometry of the widely used $\lambda/2$ dipole antenna. Because of the standing wave current pattern, it is also classified as a *standing wave* antenna. If $\ell < \lambda$, the phase of the current standing wave pattern in each arm is the same throughout its length. In addition, it is oriented spatially in the same direction as that of the other arm, as shown in Fig. 1(c). Thus the fields radiated by the two arms of the dipole (vertical parts of a flared transmission line) will primarily reinforce each other in some directions and cancel each other toward others. This results in the formation of amplitude pattern lobes which are illustrated in the later part of this paper.

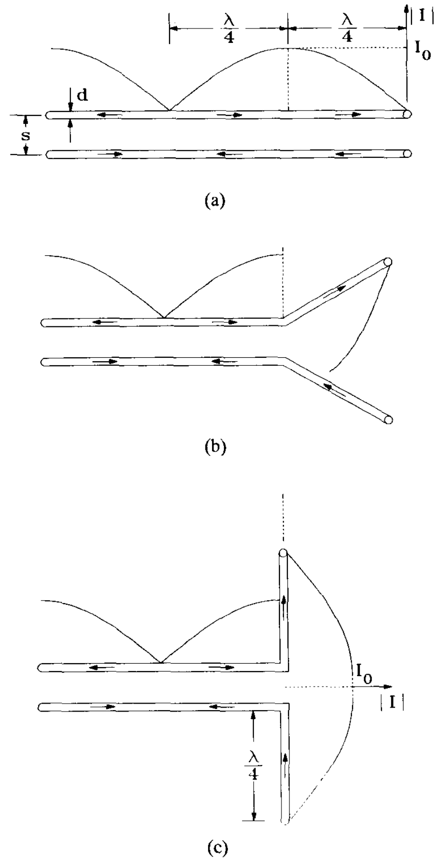

Fig. 1. Radiation from a two-wire transmission line and linear dipole. (a) Two-wire transmission line. (b) Flared transmission line. (c) Linear dipole.

B. Maxwell's Equations, the Wave Equation, and Boundary Conditions

An antenna configuration is an electromagnetic boundary-value problem. Therefore, the fields radiated must satisfy Maxwell's equations which, for a lossless medium ($\sigma = 0$) and time-harmonic fields (assuming an $e^{j\omega t}$ time convention), can be written as [33]:

$$\nabla \times \boldsymbol{E} = -\boldsymbol{M}_i - j\omega\mu\boldsymbol{H} \quad (1a)$$

$$\nabla \times \boldsymbol{H} = +\boldsymbol{J}_i + j\omega\epsilon\boldsymbol{E} \quad (1b)$$

$$\nabla \cdot (\epsilon\boldsymbol{E}) = q_{ve} \quad (1c)$$

$$\nabla \cdot (\mu\boldsymbol{H}) = q_{vm}. \quad (1d)$$

In (1a)–(1d) both electric ($\boldsymbol{J}_i$) and magnetic ($\boldsymbol{M}_i$) current densities, and electric (q_{ve}) and magnetic (q_{vm}) charge densities are allowed to represent the sources of excitation. The respective current and charge densities are related by the continuity equations

$$\nabla \cdot \boldsymbol{J}_i = -j\omega q_{ve} \quad (2a)$$

$$\nabla \cdot \boldsymbol{M}_i = -j\omega q_{vm}. \tag{2b}$$

Although magnetic sources are not physical, they are often introduced as *electrical equivalents* to facilitate solutions of physical boundary-value problems. In fact, for some configurations, both electric and magnetic equivalent current densities are used to represent actual antenna systems. For a metallic wire antenna, such as a dipole, an electric current density is used to represent the antenna. However, an aperture antenna, such as a waveguide or horn, can be represented by either an equivalent magnetic current density or by an equivalent electric current density or both. This will be demonstrated in Section IV-B.

In addition to satisfying Maxwell's equations of (1a)–(1d), the fields radiated by the antenna must satisfy the boundary conditions of [33]

$$-\hat{n} \times \boldsymbol{E}_d = \boldsymbol{M}_s \tag{3a}$$
$$\hat{n} \times \boldsymbol{H}_d = \boldsymbol{J}_s \tag{3b}$$
$$\hat{n} \cdot (\epsilon \boldsymbol{E}_d) = q_{se} \tag{3c}$$
$$\hat{n} \cdot (\mu \boldsymbol{H}_d) = q_{sm}. \tag{3d}$$

The first two equations, (3a) and (3b), enforce the boundary conditions on the discontinuity of the tangential components of the electric and magnetic fields while (3c) and (3d) enforce the boundary conditions on the discontinuity of the normal components of the electric and magnetic flux densities. In (3a)–(3d), $\boldsymbol{J}_s/\boldsymbol{M}_s$ and q_{se}/q_{sm} represent, respectively, the electric/magnetic surface current densities and electric/magnetic surface charge densities. For time-harmonic fields, all four boundary conditions of (3a)–(3d) are not independent. The first two, (3a) and (3b), form an independent and sufficient set [33].

In addition to the boundary conditions of (3a)–(3d), the solutions for the fields radiated by the antenna must also satisfy the *radiation condition* which requires in an infinite homogeneous medium that the waves travel outwardly from the source and vanish at infinity.

Since (1a) and (1b) are first-order coupled differential equations (each contains both electric and magnetic fields), it is often more desirable to uncouple the equations. When this is done, we obtain two nonhomogeneous vector wave equations; one for $\boldsymbol{E}$ and one for $\boldsymbol{H}$. These are given by [33]

$$\nabla^2 \boldsymbol{E} + \beta^2 \boldsymbol{E} = \frac{1}{\epsilon} \nabla q_{ve} + \nabla \times \boldsymbol{M}_i + j\omega\mu \boldsymbol{J}_i \tag{4a}$$
$$\nabla^2 \boldsymbol{H} + \beta^2 \boldsymbol{H} = \frac{1}{\mu} \nabla q_{vm} - \nabla \times \boldsymbol{J}_i + j\omega\epsilon \boldsymbol{M}_i \tag{4b}$$

where $\beta^2 = \omega^2 \mu\epsilon$.

For a radiation problem, the first step is to represent the antenna excitation by its source, represented in (4a) and (4b) by the current density $\boldsymbol{J}_i$ or $\boldsymbol{M}_i$ or both, having taken into account the boundary conditions. This will be demonstrated in Section IV. The next step is to solve (4a) and (4b) for $\boldsymbol{E}$ and $\boldsymbol{H}$. This is a difficult step, and it usually involves an integral with a complicated intergrand. This procedure is represented in Fig. 2 as Path 1.

To reduce the complexity of the problem, it is a common practice to break the procedure into two steps. This is represented in Fig. 2 by Path 2. The first step involves an integration while the second involves a differentiation. To accomplish this, auxiliary vector potentials are introduced. The most commonly used potentials are $\boldsymbol{A}$ (magnetic vector potential) and $\boldsymbol{F}$ (electric vector potential). Although the electric and magnetic field intensities ($\boldsymbol{E}$ and $\boldsymbol{H}$) represent physically measurable quantities, for most engineers the vector potentials are strictly mathematical tools. The Hertz vector potentials $\boldsymbol{\Pi}_e$ and $\boldsymbol{\Pi}_h$ make up another possible pair. The Hertz vector potential $\boldsymbol{\Pi}_e$ is analogous to $\boldsymbol{A}$ and $\boldsymbol{\Pi}_h$ is analogous to $\boldsymbol{F}$ [1], [33]. In the solution of a problem, only one set, $\boldsymbol{A}$ and $\boldsymbol{F}$ or $\boldsymbol{\Pi}_e$ and $\boldsymbol{\Pi}_h$, is required. In the first step of the Path 2 solution, the vector potentials $\boldsymbol{A}$ and $\boldsymbol{F}$ (or $\boldsymbol{\Pi}_e$ and $\boldsymbol{\Pi}_h$) are found, once the sources $\boldsymbol{J}_i$ and/or $\boldsymbol{M}_i$ are specified. This step involves an integration but one which is not as difficult as the integration of Path 1. The next step of the Path 2 solution is to find the fields $\boldsymbol{E}$ and $\boldsymbol{H}$, from the vector potentials $\boldsymbol{A}$ and $\boldsymbol{F}$ (or $\boldsymbol{\Pi}_e$ and $\boldsymbol{\Pi}_h$). This step involves differentiation. The equations that are essential for the solution of Path 2 will be outlined next using the vector potentials $\boldsymbol{A}$ and $\boldsymbol{F}$. The derivation can be found in many books, such as [1], [4], [7], [18], [19], [21], [33], and others.

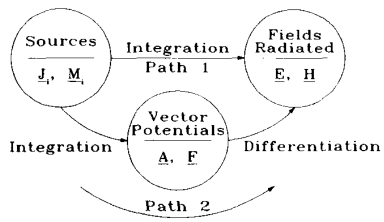

Fig. 2. Procedure to solve antenna radiation.

C. The Vector Potentials $\boldsymbol{A}$ and $\boldsymbol{F}$

In step one of Path 2, once the sources $\boldsymbol{J}_i$ and $\boldsymbol{M}_i$ are specified, the vector potentials $\boldsymbol{A}$ and $\boldsymbol{F}$ are related, respectively, to $\boldsymbol{J}_i$ and $\boldsymbol{M}_i$ by

$$\nabla^2 \boldsymbol{A} + \beta^2 \boldsymbol{A} = -\mu \boldsymbol{J}_i \tag{5a}$$
$$\nabla^2 \boldsymbol{F} + \beta^2 \boldsymbol{F} = -\epsilon \boldsymbol{M}_i. \tag{5b}$$

If the current densities are distributed over a surface S, such as that of a perfect conductor immersed in an infinite homogeneous medium, the solutions of (5a) and (5b) can be written, by referring to Fig. 3(a), as

$$\boldsymbol{A} = \frac{\mu}{4\pi} \int_S \int \boldsymbol{J}_s \frac{e^{-j\beta R}}{R} ds' \tag{6a}$$
$$\boldsymbol{F} = \frac{\epsilon}{4\pi} \int_S \int \boldsymbol{M}_s \frac{e^{-j\beta R}}{R} ds' \tag{6b}$$

where R is the distance from any point on the source to the observation point. For the solutions of (6a) and (6b), $\boldsymbol{J}_i$ and $\boldsymbol{M}_i$ in (5a) and (5b) are replaced by $\boldsymbol{J}_s$ and $\boldsymbol{M}_s$ which have the units of A/m and V/m, respectively. If the current densities are distributed over a volume, the surface integrals

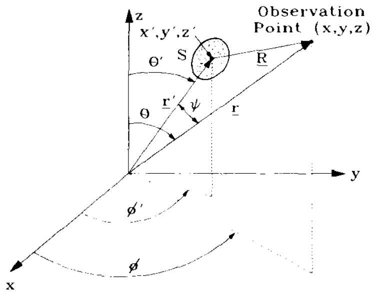

(a)

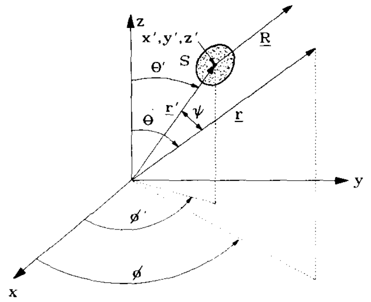

(b)

Fig. 3. Coordinate system arrangements for (a) near-field and (b) far-field radiation.

of (6a) and (6b) are replaced by volume integrals. When the currents are distributed over a thin wire, the surface integrals of (6a) and (6b) can be approximated by line integrals [1], [33].

The most difficult step in the solution of Path 2 is the evaluation of the integrals of (6a) and (6b). For most practical antenna geometries, these integrals cannot be evaluated in closed form. Usually approximations are made and/or numerical techniques are employed. With today's computer technology, numerical evaluation of integrals is a much simpler, more convenient, and more efficient procedure than in the past. Computational electromagnetics for antenna radiation are discussed in this issue in "Low-frequency computational electromagnetics for antenna analysis," by E. K. Miller and G. J. Burke.

D. The Electric and Magnetic Fields $\boldsymbol{E}$ and $\boldsymbol{H}$

Once the vector potentials $\boldsymbol{A}$ and $\boldsymbol{F}$ have been found by (6a) and (6b), the second step in the solution of Path 2 is to find the electric and magnetic fields $\boldsymbol{E}$ and $\boldsymbol{H}$. This is accomplished by using the equations [1], [33]

$$\boldsymbol{E} = \boldsymbol{E}_A + \boldsymbol{E}_F = \left[-j\omega\boldsymbol{A} - j\frac{1}{\omega\mu\epsilon}\nabla(\nabla\cdot\boldsymbol{A})\right] + \left[-\frac{1}{\epsilon}\nabla\times\boldsymbol{F}\right] \quad (7a)$$

and

$$\boldsymbol{H} = \boldsymbol{H}_A + \boldsymbol{H}_F = \left[\frac{1}{\mu}\nabla\times\boldsymbol{A}\right] + \left[-j\omega\boldsymbol{F} - j\frac{1}{\omega\mu\epsilon}\nabla(\nabla\cdot\boldsymbol{F})\right]. \quad (7b)$$

The forms of (5a)–(5b) and (7a)–(7b) are based on choosing the relationships between $\boldsymbol{A}$ & ϕ and $\boldsymbol{F}$ & ϕ of

$$\nabla\cdot\boldsymbol{A} = -j\omega\epsilon\mu\phi_e \quad (7c)$$

$$\nabla\cdot\boldsymbol{F} = -j\omega\epsilon\mu\phi_m \quad (7d)$$

which each is known as the *Lorentz condition* or *gauge* (ϕ_e and ϕ_m are scalar functions of position usually referred to as *scalar potentials.*) The choices of (7c) and (7d) were made to reduce (5a), (5b), (7a), and (7b) to their simplest forms; however, they are not the only possible choices.

In (7a) and (7b), the terms within the first brackets are the fields due to the vector potential $\boldsymbol{A}$ (and as a consequence due to electric current density) while the terms within the second brackets are the fields due to the vector potential $\boldsymbol{F}$ (and as a consequence due to magnetic current density). If either of the sources (electric or magnetic) do not exist, the corresponding electric and magnetic fields (and vector potentials $\boldsymbol{A}$ or $\boldsymbol{F}$) are set to zero. It is evident from (7a) and (7b) that superposition is used when both electric and magnetic sources are needed to represent the source of radiation.

E. Field Regions

The space surrounding an antenna is usually subdivided into three regions: the *reactive near-field region,* the *radiating near-field (Fresnel) region,* and the *far-field (Fraunhofer)* region. These regions are so designated to identify the field structure in each. Although no abrupt changes in the field configurations are noted as the boundaries are crossed, there are distinct differences among them [1], [11]. The boundaries separating these regions are not unique, although various criteria have been established and are commonly used to identify the regions. The following definitions in quotations are from [46].

The *reactive near-field region* is defined as "that region of the field immediately surrounding the antenna wherein the reactive field predominates." For most antennas, the outer boundary of this region is commonly taken to exist at a distance $R < 0.62\sqrt{D^3/\lambda}$ from the antenna, where λ is the wavelength and D is the largest dimension of the antenna.

The *radiating near-field (Fresnel) region* is defined as "that region of the field of an antenna between the reactive near-field region and the far-field region wherein radiation fields predominate and wherein the angular field distribution is dependent upon the distance from the antenna." The radial distance R over which this region exists is $0.62\sqrt{D^3/\lambda} \leq R < 2D^2/\lambda$ (provided D is large compared to the wavelength). This criterion is based on a maximum phase error of $\pi/8$ radians (22.5°) [1], [11]. In this region the field pattern is, in general, a function of the radial distance and the radial field component may be appreciable.

The *far-field (Fraunhofer) region* is defined as "that region of the field of an antenna where the angular field distribution is essentially independent of the distance from the antenna." In this region, the real part of the power density is dominant. The radial distance R over which this region exists is $R \geq 2D^2/\lambda$ (provided D is large compared to the wavelength). The outer boundary is ideally at infinity. This criterion is also based on a maximum phase error of $\pi/8$ radians (22.5°) [1], [11], [18]. In this region, the field components are essentially transverse to the radial distance, and the angular distribution is independent of the radial distance. The evaluation of the integrals in (6a) and (6b) varies according to the region where the observations are made. The evaluation is most difficult in the reactive near-field region. As the observation point is moved radially outward, approximations can be made in the integrands of (6a) and (6b) to reduce the complexity of the evaluation. The evaluation is easiest in the far-field region, and that is usually the region of most applications.

Let us outline the procedure for the evaluation of integrals for the potentials $\boldsymbol{A}$ and $\boldsymbol{F}$ as the observation point is moved to the far-field region. This will be done for the surface integrals of (6a) and (6b). As the observation point is moved radially outward, the distance R can be approximated and leads to a simplification in the evaluation of the integral.

In the far-field (Fraunhofer) region, the radial distance R of Fig. 3(a) can be approximated by [1], [33]

$$R \simeq \begin{cases} r - r' \cos\psi & \text{for phase terms} \quad (8a) \\ r & \text{for amplitude terms.} \quad (8b) \end{cases}$$

Graphically, the approximation of (8a) is illustrated in Fig. 3(b) where the radial vectors R and r are parallel to each other. Although such a relation is strictly valid only at infinity, it becomes more accurate as the observation point is moved outward at radial distances exceeding $2D^2/\lambda$. Since the far-field region extends at radial distances of $R \geq 2D^2/\lambda$, the approximation of (8a) for the radial distance R leads to phase errors which do not exceed $\pi/8$ radians (22.5°). It has been shown that such phase errors do not have a pronounced effect on the variations of the far-field amplitude patterns (at least at parts of the patterns in which the relative field strength is not lower than about 25 dB) [1], [11].

Using the approximations of (8a) and (8b) for observations in the far-field region, the integrals of (6a) and (6b) can be reduced to

$$\boldsymbol{A} \simeq \frac{\mu e^{-j\beta r}}{4\pi r} \int_S \int \boldsymbol{J}_s e^{j\beta r' \cos\psi} ds' = \frac{\mu e^{-j\beta r}}{4\pi r} \boldsymbol{N} \quad (9)$$

$$\boldsymbol{N} = \int_S \int \boldsymbol{J}_s e^{j\beta r' \cos\psi} ds' \quad (9a)$$

$$\boldsymbol{F} \simeq \frac{\epsilon e^{-j\beta r}}{4\pi r} \int_S \int \boldsymbol{M}_s e^{j\beta r' \cos\psi} ds' = \frac{\epsilon e^{-j\beta r}}{4\pi r} \boldsymbol{L} \quad (10)$$

$$\boldsymbol{L} = \int_S \int \boldsymbol{M}_s e^{j\beta r' \cos\psi} ds'. \quad (10a)$$

With the approximations of (9)–(10a), the spherical components of the electric and magnetic fields of (7a) and (7b) can be written in scalar form as [1], [33]

$$E_r \simeq 0 \quad (11a)$$

$$E_\theta \simeq -j \frac{\beta e^{-j\beta r}}{4\pi r} [L_\phi + \eta N_\theta] \quad (11b)$$

$$E_\phi \simeq j \frac{\beta e^{-j\beta r}}{4\pi r} [L_\theta - \eta N_\phi] \quad (11c)$$

$$H_r \simeq 0 \quad (12a)$$

$$H_\theta \simeq j \frac{\beta e^{-j\beta r}}{4\pi r} \left[N_\phi - \frac{L_\theta}{\eta}\right] \quad (12b)$$

$$H_\phi \simeq -j \frac{\beta e^{-j\beta r}}{4\pi r} \left[N_\theta + \frac{L_\phi}{\eta}\right] \quad (12c)$$

where η is the intrinsic impedance of the medium ($\eta = \sqrt{\mu/\epsilon}$ while N_θ, N_ϕ, and L_θ, L_ϕ are the spherical θ and ϕ components of $\boldsymbol{N}$ and $\boldsymbol{L}$ from (9a) and (10a). In antenna theory, the spherical coordinate system is the most widely used system.

By examining (11a)–(12c), it is apparent that

$$E_\theta \simeq \eta H_\phi \quad (13a)$$

$$E_\phi \simeq -\eta H_\theta. \quad (13b)$$

The relations of (13a) and (13b) indicate that in the far-field region the fields radiated by an antenna and observed in a small neighborhood on the surface of a large radius sphere have all the attributes of a plane wave whereby the corresponding electric and magnetic fields are orthogonal to each other and to the radial direction.

To use the above procedure, the sources representing the physical antenna structure must radiate into an infinite homogeneous medium. If that is not the case, then the problem must be reduced further (e.g., though the use of a theorem, such as the image theorem) until the sources radiate into an infinite homogeneous medium. This again will be demonstrated in Section IV-A for the analysis of the aperture antenna.

IV. Antenna Source Modeling

The first step in the analysis of the fields radiated by an antenna is the specification of the sources to represent the antenna. Here we will present two examples of source modeling; one for a thin wire antenna (such a dipole) and the other for an aperture antenna (such as a waveguide). These are two distinct examples each with a different source modeling; the wire requires an electric current density while the aperture is represented by an equivalent magnetic current density.

A. Wire Source Modeling

Let us assume that the wire antenna is a dipole, as shown in Fig. 4. If the wire has circular cross section with radius a, the electric current density induced on the surface of the wire will be symmetrical about the circumference (no ϕ variations). If the wire is also very thin ($a \ll \lambda$), it is common to assume that the excitation source representing

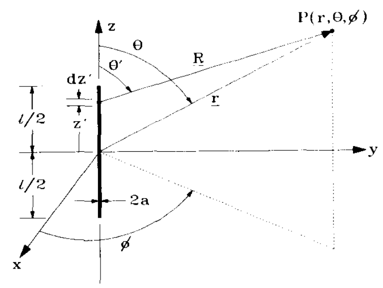

Fig. 4. Dipole geometry for electromagnetic wave radiation.

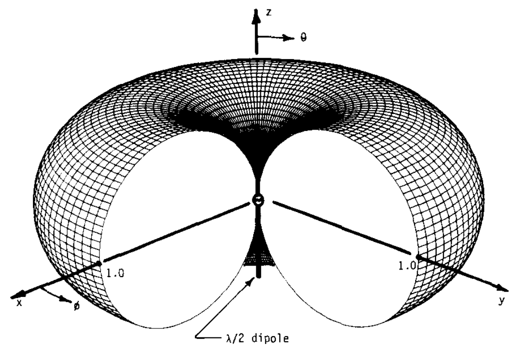

Fig. 5. Three-dimensional amplitude radiation pattern of a $\lambda/2$ dipole.

the antenna is a current along the axis of the wire. This current must vanish at the ends of the wire, and for very thin wires assumes a sinusoidal distribution. For a center-fed dipole, this excitation is often represented by

$$\boldsymbol{I}_e = \begin{cases} \hat{a}_z I_0 \sin\left[\beta((\ell/2) - z')\right] & 0 \le z' \le \ell/2 \quad (14a) \\ \hat{a}_z I_0 \sin\left[\beta((\ell/2) + z')\right] & -\ell/2 \le z' \le 0. \quad (14b) \end{cases}$$

No magnetic source representation is necessary for this type of an antenna. The fields radiated by the antenna can now be found by first determining the potential $\boldsymbol{A}$ using (6a), where the surface integral is reduced to a line integral, and in turn the fields are determined by (7a) and (7b). For observations in the far-field region, the approximations of (8a) and (8b) can be used. When this is done, it can be shown by also using (9)–(12c) that the electric and magnetic fields can be written as

$$E_\theta \simeq j\eta \frac{I_0 e^{-j\beta r}}{2\pi r}\left[\frac{\cos(\beta\ell/2\cos\theta) - \cos(\beta\ell/2)}{\sin\theta}\right] \quad (15a)$$

$$H_\phi \simeq \frac{E_\theta}{\eta}. \quad (15b)$$

To illustrate the field variations of (15a), a three-dimensional graph of the normalized field amplitude pattern for a half-wavelength ($\ell = \lambda/2$) dipole is plotted in Fig. 5 using software from [47]. A 90° angular section of the pattern has been omitted to illustrate the figure-eight elevation plane pattern variation. As the length of the wire increases, the pattern becomes narrower. When the length exceeds one wavelength ($\ell > \lambda$), sidelobes are introduced into the elevation plane pattern [1].

B. Aperture Source Modeling

To analyze aperture antennas, the most often used procedure is to model the source representing the actual antenna by the *Field Equivalence Principle (FEP)*, also referred to as *Huygen's Principle* [1], [18], [19], [21], [33]. With this method, the actual antenna is replaced by equivalent sources that, externally to a closed surface enclosing the actual antenna, produce the same fields as those radiated by the actual antenna. This procedure is analogous to the Thevenin Equivalent of circuit analysis which produces the same response, to an external load, as the actual circuit.

The FEP requires that first an imaginary surface is chosen which encloses the actual antenna. This is shown dashed in Fig. 6(a). Once the imaginary closed surface is chosen, one of the equivalents of the FEP requires that the volume within the closed surface be replaced by a perfect electric conductor (PEC) and an equivalent magnetic current density source placed over the entire surface of the conductor, as shown in Fig. 6(b). To insure equivalence, the magnetic current density source over the closed surface must be equal to

$$\boldsymbol{J}_s = \hat{n} \times \boldsymbol{H}_s \quad (16a)$$

$$\boldsymbol{M}_s = -\hat{n} \times \boldsymbol{E}_s \quad (16b)$$

where $\hat{n}$ is a unit vector normal to the surface and $\boldsymbol{E}_s$, $\boldsymbol{H}_s$ are the electric and magnetic fields produced by the actual antenna on the chosen closed surface. Therefore, to form $\boldsymbol{J}_s$ by (16) and $\boldsymbol{M}_s$ by (17), the tangential components of the magnetic and electric fields due to the actual antenna must be known over the chosen imaginary closed surface. Since $\boldsymbol{J}_s$ of (16) is tangent to the PEC, it is shorted out and it produces no radiation. Therefore, using the equivalent of Fig. 6(b), $\boldsymbol{J}_s$ does not contribute and it can be set to zero, as shown in Fig. 6(b). The critical step here is to choose the imaginary closed surface so that $\boldsymbol{M}_s$ can be formed everywhere on it. Often the closed surface is chosen so that $\boldsymbol{M}_s$ is finite over a limited area of the surface and zero elsewhere.

The equivalent problem now is to determine the fields radiated by a magnetic current density next to a PEC. The procedure outlined in Section III cannot be used here, because the source does not radiate into an infinite homogeneous medium (the PEC is present). Therefore, a further equivalent reduction of the problem must be performed. It may seem that the equivalent problem of Fig. 6(b) is no simpler than the actual problem. However, in some cases, it can be solved exactly while in others it suggests useful approximations. This will be demonstrated by the example that follows.

Another equivalence of the FEP requires that the volume within the closed surface be replaced by a perfect magnetic conductor (PMC) with equivalent electric and magnetic current density sources over its entire closed surface, as

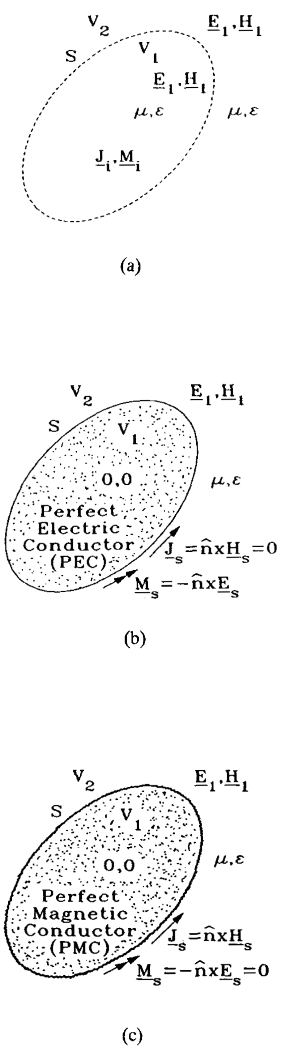

Fig. 6. Electric and magnetic conductor field equivalents for radiation. (a) Actual antenna system. (b) Electric conductor equivalent. (c) Magnetic conductor equivalent.

shown in Fig. 6(c). A PMC, although nonphysical, is often used as an equivalent medium and requires that the tangential components of the magnetic field vanish on its surface. To insure equivalence, the electric and magnetic current densities must be equal to (16) and (17). Therefore, to form $\boldsymbol{J}_s$ by (16) and $\boldsymbol{M}_s$ by (17), the tangential components of the magnetic and electric fields radiated by the antenna must be known. Since $\boldsymbol{M}_s$ of (17) is tangent to the PMC, it is shorted out and it produces no radiation. Therefore, using the equivalent of Fig. 6(c), $\boldsymbol{M}_s$ does not contribute and it can be set to zero, as shown in Fig. 6(c).

The choice of whether to use the magnetic current density equivalent of (17) and Fig. 6(b) or the electric current density equivalent of (16) and Fig. 6(c) as the FEP equivalent is left to the investigator. However, a judicious choice can significantly simplify the analysis. This is demonstrated by the example that follows. Once the FEP equivalent choice is made, the next step is to find $\boldsymbol{A}$ or $\boldsymbol{F}$ using (6a) or (6b) and then to find the fields using (7a) and (7b). For far-field observations, the approximations of (9)–(13b) can be used in lieu of (6a)–(7b).

To demonstrate the procedure, let us assume that an open-ended rectangular waveguide aperture mounted on an infinite planar PEC radiates on a semi-infinite homogeneous medium, as shown in Fig. 7(a). Let us assume that the fields in the waveguide aperture are those of the dominant TE_{10} mode. Hence, the tangential electric field over the x–y plane is

$$\boldsymbol{E}_s = \begin{cases} \hat{a}_y E_0 \cos(\frac{\pi}{a}x') & -a/2 \le x' \le a/2 \\ & -b/2 \le y' \le b/2 \quad (18a) \\ 0 & \text{elsewhere over the PEC.} \quad (18b) \end{cases}$$

By adopting the FEP equivalent of Fig. 6(b), an imaginary closed surface is chosen to coincide with the infinite PEC (x–y plane) and covers also the waveguide aperture. The imaginary closed surface is chosen to coincide with the x–y plane because the tangential components of the electric field, and thus the equivalent magnetic current density, are nonzero only in the aperture. Using (17) and (18a)–(18b), we can write

$$\boldsymbol{M}_s = -\hat{n} \times \boldsymbol{E}_s = \begin{cases} \hat{a}_x E_0 \cos((\pi/a)x') & -a/2 \le x' \le a/2 \\ & -b/2 \le y' \le b/2 \quad (19a) \\ 0 & \text{elsewhere over the PEC.} \quad (19b) \end{cases}$$

The equivalent problem to solve now is that shown in Fig. 6(b); i.e., the magnetic current density of (19a) and (19b) next to the PEC. Using image theory, the equivalent of Fig. 6(b) is replaced by a magnetic current density of twice the strength of (19a) radiating into an infinite homogeneous medium, as shown in Fig. 7(b). Now using (9)–(12c), the far-field electric and magnetic fields radiated by the waveguide can be written as [1]

$$E_r \simeq H_r \simeq 0 \quad (20a)$$

$$E_\theta \simeq -\frac{\pi}{2} C \sin\phi \frac{\cos(X)}{(X)^2 - (\frac{\pi}{2})^2} \frac{\sin(Y)}{Y} \quad (20b)$$

$$E_\phi \simeq -\frac{\pi}{2} C \cos\theta \cos\phi \frac{\cos(X)}{(X)^2 - (\pi/2)^2} \frac{\sin(Y)}{Y} \quad (20c)$$

$$H_\theta \simeq -\frac{E_\phi}{\eta} \quad (20d)$$

$$H_\phi \simeq +\frac{E_\theta}{\eta} \quad (20e)$$

$$X = \frac{\beta a}{2} \sin\theta \cos\phi \quad (20f)$$

$$Y = \frac{\beta b}{2} \sin\theta \sin\phi \quad (20g)$$

$$C = j \frac{ab\beta E_0 e^{-j\beta r}}{2\pi r}. \quad (20h)$$

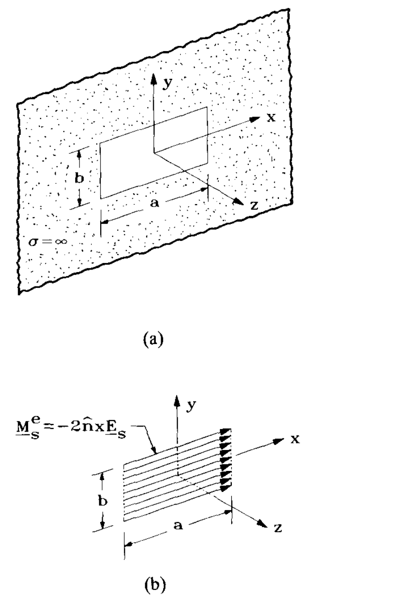

Fig. 7. (a) Waveguide aperture on an infinite ground plane and (b) its equivalent.

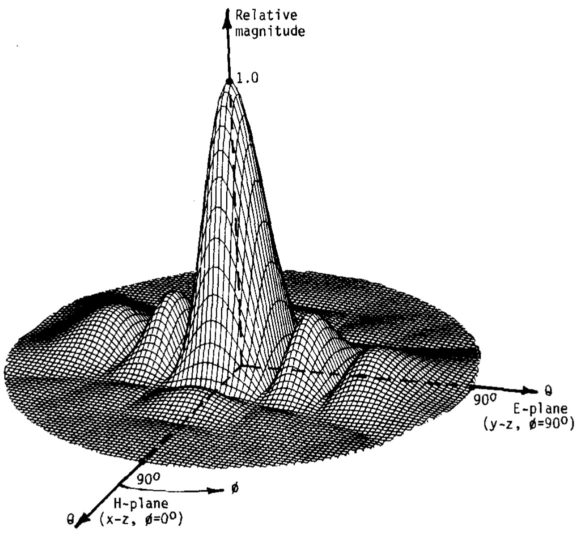

Fig. 8. Three-dimensional amplitude radiation pattern for an aperture ($a = 3\lambda, b = 3\lambda$) on an infinite ground plane.

A three-dimensional normalized field pattern of a rectangular aperture with dimensions of $a = 3\lambda$ and $b = 3\lambda$ is shown in Fig. 8. The minor lobes formed throughout the space are clearly shown.

V. Antenna Parameters and Figures-of-Merit

There are many parameters and figures-of-merit that characterize the performance of an antenna system. The definitions of these can be found in [1], [46], and those used here from [46] are found in quotation marks. Because of limited space, some of the most important are included here.

An *antenna pattern* is defined as a graphical representation, usually in the far-field region, of one of the antenna's parameters. For a complete description, the parameters of interest are usually plotted as a function of the spherical directional angles θ, ϕ. Parameters of interest include amplitude, phase, polarization, and directivity. An amplitude pattern is usually comprised of a number of lobes.

A *main (major) lobe* is defined as "the radiation lobe containing the direction of maximum radiation. In certain antennas, such as multilobed or split-beam antennas, there may exist more than one major lobe."

A *side lobe* is defined as "a radiation lobe in any direction other than that of the major lobe." The amplitude level of a side lobe relative to the main lobe (usually expressed in decibels) is referred to as *side lobe level.*

It is instructive in characterizing antenna operation and performance to use circuit equivalents. For the antenna system of Fig. 9(a), two of the simplest are those of Fig. 9(b) and (c) representing, respectively, the Thevenin equivalent of the antenna in the transmitting and receiving modes. The resistance R_r is referred to as the *radiation resistance*, and it is this resistance that represents antenna radiation or scattering. The radiation resistance is part of the antenna impedance whose imaginary part is represented by X_A. The conductive and dielectric losses of the antenna are accounted by R_L while the impedance of the generator and receiver (load) are represented, respectively, by $Z_g = R_g + jX_g$ and $Z_T = R_T + jX_T$.

Input Impedance is defined as "the impedance presented by an antenna at its terminals." It is expressed at the terminals as the ratio of the voltage to current or the ratio of the appropriate components of the electric to magnetic fields, and it is usually complex. When the antenna impedance Z_A of Fig. 9(a) is referred to the input terminals of the antenna, it reduces to the input impedance [1].

Radiation efficiency is defined as "the ratio of the total power radiated by an antenna to the net power accepted by an antenna from the connected transmitter." Using the equivalent circuit of Fig. 9(b) and (c), it can be written as

$$e_r = \frac{R_r}{R_r + R_L} \tag{21}$$

where R_r = radiation resistance R_L = loss resistance.

Power density S is defined as the power density (W/m^2) of the fields radiated by the antenna. In general, the power density is complex. In the reactive near-field, the imaginary component is dominant. In the far-field, the real part is dominant. In equation form, the power density $\boldsymbol{S}$ is expressed as [1]

$$\boldsymbol{S} = \frac{1}{2}\boldsymbol{E} \times \boldsymbol{H}^* = \boldsymbol{S}_r + j\boldsymbol{S}_i \tag{22}$$

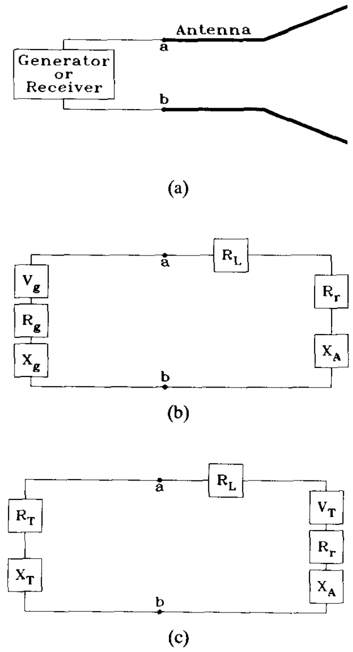

Fig. 9. Thevenin equivalents for transmitting and receiving antennas. (a) Antenna system. (b) Thevenin equivalent: transmitting. (c) Thevenin equivalent: receiving.

where $\boldsymbol{E}$ and $\boldsymbol{H}$ are the fields radiated by the antenna ($*$ indicates complex conjugate). The real part is usually referred to as *radiation density.*

Radiation intensity U is defined as "the power radiated from an antenna per unit solid angle (steredian)." The radiation intensity is usually determined in the far field, and it is related to the real part of the power density by

$$U = r^2 S_r \tag{23}$$

where r is the spherical radial distance.

Beamwidth is defined as the angular separation between two directions in which the radiation intensity is identical, with no other intermediate points of the same value. When the intensity is one-half of the maximum, it is referred to as *half-power beamwidth.*

An *isotropic radiator* is defined as "a hypothetical, lossless antenna having equal radiation intensity in all directions." Although such an antenna is an idealization, it is often used as a convenient reference to express the directive properties of actual antennas. Its radiation density S_{r0} and intensity U_0 are defined, respectively, as

$$S_{r0} = \frac{P_r}{4\pi r^2} \tag{24a}$$

$$U_0 = \frac{P_r}{4\pi} \tag{24b}$$

where P_r represents the power radiated by the antenna.

Directivity is one of the most important figures-of-merit that describes the performance of an antenna. It is defined as "the ratio of the radiation intensity in a given direction from the antenna to the radiation intensity averaged over all directions." Using (24b), it can be written as

$$D = \frac{U(\theta,\phi)}{U_0} = \frac{4\pi U(\theta,\phi)}{P_r} \tag{25}$$

where $U(\theta,\phi)$ is the radiation intensity in the direction θ,ϕ and P_r is the radiated power. If the direction is not specified, it implies the direction of maximum radiation intensity (maximum directivity) expressed as

$$D_0 = \frac{U_m(\theta,\phi)}{U_0} = \frac{4\pi U_m(\theta,\phi)}{P_r}. \tag{25a}$$

The directivity is an indicator of the relative directional properties of the antenna. As defined in (25) and (25a), the directional properties of the antenna in question are compared to those of an isotropic radiator. Sometimes this comparison is made relative to another standard radiator whose directivity (relative to an isotropic radiator) is known (like a $\lambda/2$ dipole or a standard gain horn). This allows us to relate the directivity of the element in question to that of an isotropic radiator by simply adding (if expressed in decibels) the relative directivities of one element to another. This procedure is analogous to that used to determine the overall gain of cascaded amplifiers.

To demonstrate the significance of directivity, let us examine the directivity of a half-wavelength dipole ($\ell = \lambda/2$) approximated as

$$D \simeq 1.67 \sin^3\theta \tag{26}$$

where θ is measured from the axis along the length of the dipole. The values represented by (26) and those of an isotropic source ($D = 1$) are plotted three-dimensionally in Fig. 10. At each point, only the largest value of the two directivities is plotted. It is apparent that when $\sin^{-1}(1/\sqrt{1.67}) = 57.44^\circ \leq \theta \leq 122.56^\circ$, the dipole radiator has greater directivity (greater intensity concentration) in those directions than that of an isotropic source. Outside this range of angles, the isotropic radiator has higher directivity (more intense radiation). The maximum directivity of the dipole (relative to the isotropic radiator) occurs when $\theta = \pi/2$, and it is 1.67 (or 2.23 dB). It simply means that at $\theta = 90^\circ$ the dipole radiation is 2.23 dB more intense than that of the isotropic radiator (with the same radiated power).

Gain is probably the most important figure-of-merit of an antenna. It is defined as "the ratio of the radiation intensity in a given direction, to the radiation intensity that would be obtained if the power accepted by the antenna were radiated isotropically." Using (24b), it can be written as

$$G = \frac{U(\theta,\phi)}{U_a} = \frac{4\pi U(\theta,\phi)}{P_a} \tag{27}$$

where P_a is the accepted (input) power to the antenna. If the direction is not specified, it implies the direction of maximum radiation (maximum gain). In simplest terms, the main difference between the definitions of directivity, as given by (25), and gain, as given by (27), is that the directivity is based on the radiated power while the gain

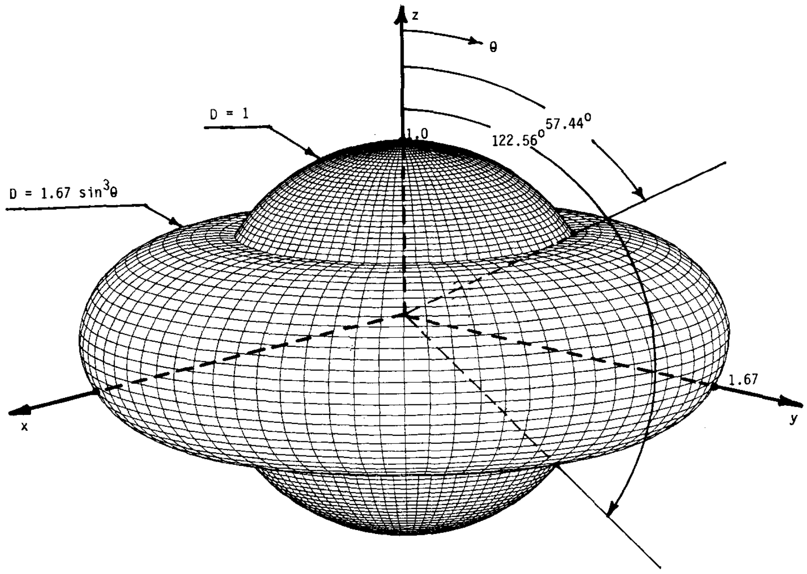

Fig. 10. Three-dimensional directivity pattern for a $\lambda/2$ dipole and an isotropic source.

is based on the accepted (input) power. Since all of the accepted (input) power is not radiated (because of losses), the two are related by

$$P_r = e_r P_a \tag{28}$$

where e_r is the radiation efficiency of the antenna as defined by (21). By using (25)–(28) the gain can be expressed as

$$G = e_r \frac{4\pi U(\theta, \phi)}{P_r} = e_r D. \tag{29}$$

For a lossless antenna, its gain is equal to its directivity.

Vector effective length (height) $\boldsymbol{h}_e$ for an antenna is a complex vector quantity represented by

$$\boldsymbol{h}_e(\theta, \phi) = \hat{a}_\theta h_\theta(\theta, \phi) + \hat{a}_\phi h_\phi(\theta, \phi) \tag{30}$$

and it is related to the far zone electric field $\boldsymbol{E}$ radiated by the antenna, with current I_{in} in its terminals, by [48]

$$\boldsymbol{E} = \hat{a}_\theta E_\theta + \hat{a}_\phi E_\phi = -j\eta \frac{\beta I_{\text{in}}}{4\pi r} \boldsymbol{h}_e e^{-j\beta r}. \tag{30a}$$

The effective height represents the antenna in the transmitting and receiving modes, and it is particularly useful in relating the open-circuit voltage V_{oc} of receiving antennas. This relation can be expressed as

$$V_{oc} = \boldsymbol{E}^i \cdot \boldsymbol{h}_e \tag{31}$$

where

- V_{oc} open-circuit voltage at antenna terminals,
- $\boldsymbol{E}^i$ incident electric field,
- $\boldsymbol{h}_e$ vector effective length.

In (31) V_{oe} can be thought as the voltage induced in a linear antenna of length $\ell = h_e$ when $\boldsymbol{h}_e$ and $\boldsymbol{E}^i$ are linearly polarized [21].

For the dipole antenna of Fig. 4 with length $\ell < \lambda/10$ whose current distribution can be approximated by triangular distribution and whose far zone electric field is given by

$$\boldsymbol{E}^i \simeq \hat{a}_\theta j\eta \frac{\beta I_0 \ell e^{-j\beta r}}{8\pi r} \sin\theta \tag{32}$$

the effective length is

$$\boldsymbol{h}_e = -\hat{a}_\theta \frac{\ell}{2} \sin\theta. \tag{32a}$$

The maximum value of the effective length of this antenna is 50% of its actual length. The maximum value of the effective length of a $\lambda/2$ dipole is $200/\pi \simeq 63.66\%$ of its actual length. The maximum effective length of an element with a uniform current distribution is 100% of its actual length ($h = \ell$). It is apparent then that the effective length of an antenna element depends largely upon the direction of wave incidence and the source distribution supported by the wave structure.

Antenna polarization in a given direction is determined by the polarization of the fields radiated by the antenna. In general, the polarization of an antenna is classified as linear, circular or elliptical. Although linear and circular polarizations are special cases of elliptical, in practice they are usually treated separately. Circular and elliptical polarizations also are classified according to the rotation of the transmitted field vectors; this rotation can be either clockwise (right-hand) or counterclockwise (left-hand) as viewed in the direction of propagation.

Polarization efficiency (polarization mismatch or loss factor) is defined as "the ratio of the power received by an antenna from a given plane wave of arbitrary polarization to the power that would be received by the same antenna from a plane wave of the same power flux density and direction of propagation, whose state of polarization has been adjusted for a maximum received power." This is an important factor that must be included in the power budget of communications systems, and it is one that sometimes is neglected. Expressed in decibels, the polarization efficiency p can be written as

$$p(\text{dB}) = 10 \log_{10} \left[\frac{|\boldsymbol{h}_e \cdot \boldsymbol{E}^{\text{inc}}|^2}{|\boldsymbol{h}_e|^2 |\boldsymbol{E}^{\text{inc}}|^2} \right] \tag{33}$$

where

$\boldsymbol{h}_e$ vector effective length,
$\boldsymbol{E}^{\text{inc}}$ incident electric field.

Effective area in a given direction is defined as "the ratio of the available power at the terminals of a receiving antenna to the power flux density of a plane wave incident on the antenna from that direction, *the wave being polarization matched to the antenna.* If the direction is not specified, the direction of maximum radiation intensity is implied." Its maximum value is related to the antenna gain by

$$A_{\text{em}} = pq \frac{\lambda^2}{4\pi} G_0 \tag{34}$$

where G_0 is the maximum gain of the antenna. In (34), p is the polarization loss factor of (33) and q is the impedance matching efficiency between the transmission line and the antenna defined as

$$q = \left(1 - |\Gamma_{\text{in}}|^2\right) \tag{35}$$

where Γ_{in} is the reflection coefficient at the input terminals of the antenna. When multiplied by the power density of the incident wave that impinges upon the antenna, the maximum effective area determines the maximum power that is delivered to a matched load connected to the antenna.

Aperture efficiency, usually expressed in percent, is defined as the ratio of the antenna's maximum effective aperture to its physical aperture which can also be expressed on the ratio of the maximum directivity of the aperture to its standard directivity, or

$$\epsilon_{\text{ap}} = \frac{A_{\text{em}}}{A_p} = \frac{D_0}{D_s} \tag{36}$$

where

A_p physical area of the antenna,
D_s standard directivity of antenna ($4\pi A_p/\lambda^2$ when $A_p >> \lambda^2$ and with radiation confined to a half space).

For a rectangular aperture mounted on an infinite ground plane and with a triangular aperture field distribution, its aperture efficiency is 75%. However, for an aperture with a sinusoidal aperture distribution, its aperture efficiency is 81%. Again we see that the aperture distribution, which satisfies the wave equation and the boundary conditions of the structure, determines its aperture efficiency. If an aperture could support a uniform field distribution, its aperture efficiency would be 100%.

VI. Antenna Theorems

A number of theorems are associated with antenna theory. Some of the most important are those of *duality, image*, and *reciprocity*. They are used to aid in the solution of antenna problems. Each of these will be outlined and related to antennas.

A. Duality Theorem

When two equations that describe the behavior of two different variables are of the same mathematical form, their solutions are also identical. The variables in the two equations that occupy identical positions are known as *dual* quantities and a solution of one can be formed by a systematic interchange of symbols to the other, provided the boundary conditions for the two problems are dual. This concept is known as the *duality theorem.*

To demonstrate the theorem, let us assume that an antenna under investigation is represented, according to Fig. 2, by current densities $\boldsymbol{J}_i \neq 0, \boldsymbol{M}_i = 0$. The equations that must be satisfied for this problem are those shown on the left column of Table 1. For another antenna, represented by current densities $\boldsymbol{J}_i = 0, \boldsymbol{M}_i \neq 0$, the equations that must be satisfied are those shown on the right column of Table 1. Comparing the respective equations in the two columns, it is evident that the equations are dual as well as their variables. The solution to one of the antennas, represented by the equations on the left (right) columns of Table 1, can be obtained from the solution of another antenna represented by the equations on the right (left) columns, and vice versa. This can be accomplished by a proper interchange of the quantities in the solution of one to obtain the solution of the other. The respective quantities, referred to as dual quantities, that must be interchanged are shown listed in Table 2. This is analogous to the duality theorem of circuits. An application of the duality theorem is in the analysis of an infinitesimal magnetic dipole whose equations and fields are the duals of those of an infinitesimal linear electric dipole, and vice versa. The infinitestimal magnetic dipole is equivalent to a small electric loop of radius a and constant electric current.

B. Image Theorem

To use the formulations outlined in Section III in the analysis of an antenna, the element must be radiating into an infinite homogeneous medium. In practice, such an environment is not available but sometimes can be approximated. The most common obstacle that is always present, even in the absence of anything else, is the ground. Any energy from the radiating element directed toward the

Table 1 Dual Equations for Electric ($\boldsymbol{J}_i$) and Magnetic ($\boldsymbol{M}_i$) Current Density Sources

Electric Sources ($\boldsymbol{J}_i \neq, \boldsymbol{M}_i = 0$)	Magnetic Sources ($\boldsymbol{J}_i = 0, \boldsymbol{M}_i \neq 0$)
$\nabla \times \boldsymbol{E}_A = -j\omega\mu \boldsymbol{H}_A$	$\nabla \times \boldsymbol{H}_F = j\omega\varepsilon \boldsymbol{E}_F$
$\nabla \times \boldsymbol{H}_A = \boldsymbol{J}_i + j\omega\varepsilon \boldsymbol{E}_A$	$-\nabla \times \boldsymbol{E}_F = \boldsymbol{M}_i + j\omega\mu \boldsymbol{H}_F$
$\nabla^2 \boldsymbol{A} + \beta^2 \boldsymbol{A} = -\mu \boldsymbol{J}_i$	$\nabla^2 \boldsymbol{F} + \beta^2 \boldsymbol{F} = -\varepsilon \boldsymbol{M}_i$
$\boldsymbol{A} = \mu/4\pi \iiint_V \boldsymbol{J}_i(e^{-j\beta R}/R)dv'$	$\boldsymbol{F} = \varepsilon/4\pi \iiint_V \boldsymbol{M}_i(e^{-j\beta R}/R)dv'$
$\boldsymbol{H}_A = 1/\mu \nabla \times \boldsymbol{A}$	$\boldsymbol{E}_F = -1/\varepsilon\ \nabla \times \boldsymbol{F}$
$\boldsymbol{E}_A = -j\omega\boldsymbol{A}\ - j(1/\omega\mu\varepsilon)\ \nabla(\nabla \cdot \boldsymbol{A})$	$\boldsymbol{H}_F = -j\omega\boldsymbol{F}\ - j(1/\omega\mu\varepsilon)\ \nabla(\nabla \cdot \boldsymbol{F})$

Table 2 Dual Quantities for Electric ($\boldsymbol{J}_i$) and Magnetic ($\boldsymbol{M}_i$) Current Density Sources

Electric Sources ($\boldsymbol{J}_i \neq, \boldsymbol{M}_i = 0$)	Magnetic Sources ($\boldsymbol{J}_i = 0, \boldsymbol{M}_i \neq 0$)
$\boldsymbol{E}_A$	$\boldsymbol{H}_F$
$\boldsymbol{H}_A$	$-\boldsymbol{E}_F$
$\boldsymbol{J}_i$	$\boldsymbol{M}_i$
$\boldsymbol{A}$	$\boldsymbol{F}$
ε	μ
μ	ε
β	β
η	$1/\eta$
$1/\eta$	η

ground will undergo reflection. The amount of reflected energy and its direction are dependent upon the geometry and electrical properties of the ground.

When dealing with antennas radiating in the presence of obstacles, image theory can sometimes be used to reduce the actual problem to an equivalent that will have sources radiating in an infinite homogeneous medium and aid toward the solution. Ideally, the electrical equivalent problem must produce outside the obstacle the same field as the actual problem. Often this procedure is used to obtain approximate but accurate solutions. To accomplish this, virtual sources (images) are introduced to replace the obstacles and account for the reflections from their surfaces. The number of images, and magnitude and phase of each depend upon the configuration and electrical properties of the obstacles.

The ideal obstacle is an infinite planar PEC ($\sigma = \infty$). In Fig. 11(a), electric and magnetic sources are located a height $\boldsymbol{h}$ above an infinite PEC. Shown in Fig. 11(b) are the orientation and position of images that must be used below the interface, to replace the conductor and account for the reflections from its surface [1], [33]. For each source above the conductor, the equivalent system comprises two sources; one (the actual source) a height $\boldsymbol{h}$ above the interface and the other (the image) at depth $\boldsymbol{h}$ below the interface. In the equivalent system of Fig. 11(b), both the source and image radiate in the same medium as the one above the conductor. This equivalent array of two sources produces the same field on and above the interface as the actual problem, but it does not lead to the correct solution of the actual problem below the interface. However, the solution within the conductor is known *a priori* ($\boldsymbol{E} = \boldsymbol{H} = 0$, because the medium is a PEC). This method of analysis is analogous to the Thevenin equivalent of circuit theory which produces the correct response to an external load, but not within the circuit it replaces, as the actual circuit. Similarly, the image theorem of Fig. 11(a) produces the same response on and above the interface as the actual physical problem, but not within the conductor.

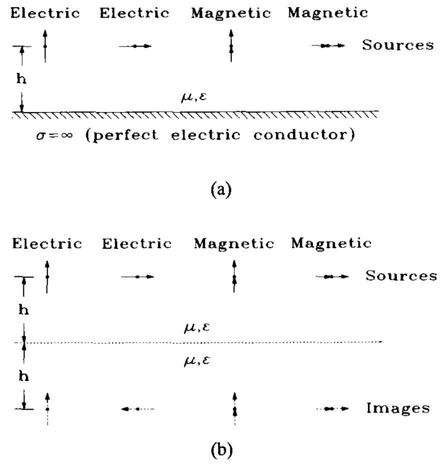

Fig. 11. Electric and magnetic sources, and their images, for a PEC interface. (a) Sources and ground plane. (b) Equivalent: sources and images.

As nonphysical magnetic sources are introduced as equivalents to replace physical radiating systems, nonphysical magnetic conductors (on which tangential magnetic fields vanish next to their surface, $\hat{n} \times \boldsymbol{H} = 0$) often are introduced as equivalent conductors. Electric and magnetic sources, each a height $\boldsymbol{h}$ above an infinite PMC, and their images at a depth $\boldsymbol{h}$ below the interface can be found in [1] and [33].

C. Reciprocity Theorem

Just as there is a reciprocity theorem in circuit theory, there is also one in antenna theory. It is a widely used relation, and its derivation is based on Maxwell's equations.

Let us assume that within a linear and isotropic (but not necessarily homogeneous) medium there exist two sets of sources $\boldsymbol{J}_1, \boldsymbol{M}_1$ and $\boldsymbol{J}_2, \boldsymbol{M}_2$ that are allowed to radiate simultaneously or individually inside the same medium at the same frequency and produce fields $\boldsymbol{E}_1, \boldsymbol{H}_1$ and $\boldsymbol{E}_2, \boldsymbol{H}_2$, respectively. It can be shown [1], [18], [19], [21], [33] that the sources and fields of the two sets satisfy

$$-\nabla \cdot (\boldsymbol{E}_1 \times \boldsymbol{H}_2 - \boldsymbol{E}_2 \times \boldsymbol{H}_1) = \boldsymbol{E}_1 \cdot \boldsymbol{J}_2 + \boldsymbol{H}_2 \cdot \boldsymbol{M}_1 - \boldsymbol{E}_2 \cdot \boldsymbol{J}_1 - \boldsymbol{H}_1 \cdot \boldsymbol{M}_2 \quad (37)$$

which is called the *Lorentz Reciprocity Theorem* in differential form.

Taking a volume integral of both sides of (37) over a volume V with surface S sufficiently large to enclose the sources of both sets, and using the divergence theorem on the left side, we can write (37) as

$$-\oiint_S (\boldsymbol{E}_1 \times \boldsymbol{H}_2 - \boldsymbol{E}_2 \times \boldsymbol{H}_1) \cdot ds = \iiint_V (\boldsymbol{E}_1 \cdot \boldsymbol{J}_2 + \boldsymbol{H}_2 \cdot \boldsymbol{M}_1 - \boldsymbol{E}_2 \cdot \boldsymbol{J}_1 - \boldsymbol{H}_1 \cdot \boldsymbol{M}_2) dv \quad (38)$$

which is designated as the *Lorentz Reciprocity Theorem* in integral form.

If the surface of integration is a sphere of infinite radius, the fields radiated by the sources when observed at very large distances (ideally at infinity) are outgoing spherical waves which satisfy the relations of (13a) and (13b). When these relations are used in the evaluation of (38), its left side vanishes and (38) reduces to

$$\iiint_V (\boldsymbol{E}_1 \cdot \boldsymbol{J}_2 - \boldsymbol{H}_1 \cdot \boldsymbol{M}_2) dv = \iiint_V (\boldsymbol{E}_2 \cdot \boldsymbol{J}_1 - \boldsymbol{H}_2 \cdot \boldsymbol{M}_1) dv. \quad (39)$$

The reciprocity theorem as expressed by (39) is the most useful form, and it is used, as is reciprocity in circuit theory, to establish various important relations.

In antenna theory, one of the applications of the reciprocity theorem of (39) is used to establish a fundamental relation between the transmitting and receiving patterns of an antenna radiating into a medium that is linear and isotropic. Assume two antennas, #1 and #2, are separated from each other. In one case, antenna #1 represented by the set of sources $(\boldsymbol{J}_1, \boldsymbol{M}_1)$, is transmitting while antenna #2 is receiving. In the other case, antenna #2, represented by sources $(\boldsymbol{J}_2, \boldsymbol{M}_2)$, is transmitting while #1 is receiving. Treating these two antennas as a two-port network, each port representing one of the antennas, it can be shown that the mutual (transfer) impedances between these two ports (antennas) are identical ($Z_{12} = Z_{21}$). This equality is used to establish that *the transmitting and receiving patterns of any antenna are identical*, provided the antenna is radiating into a medium that is linear and isotropic. Because of space limitations, the derivation of this relation will not be included here but can be found in [1], [18], [19], [21].

VII. Arrays

Specific radiation pattern requirements usually cannot be achieved by a single antenna element, because single elements usually have relatively wide radiation patterns and low values of directivity. To design antennas with very large directivities, it is usually necessary to increase the electrical size of the antenna. This can be accomplished by enlarging the electrical dimensions of the chosen single element. However, mechanical problems are usually associated with very large elements.

An alternative way to achieve large directivities, without increasing the size of the individual elements, is to use multiple single elements to form an *array* [1], [8], [14], [15], [18]–[23]. An array is really a sampled version of a very large single element. In an array, the mechanical problems of large single elements are traded for the electrical problems associated with the feed networks of arrays. However, with today's solid state technology, very efficient and low-cost feed networks can be designed.

Arrays are the most versatile antenna systems. They find wide applications not only in many space-borne systems, but in many Earth bound missions as well. In most cases, the elements of an array are identical; this is not necessary, but it is often more convenient, simpler and more practical. With arrays, it is practical to not only synthesize almost any desired amplitude radiation pattern, but the main lobe can be scanned by controlling the relative phase excitation between the elements. This is most convenient for applications where the antenna system is not readily accessible, especially for space borne missions. The beamwidth of the main lobe along with the side lobe level can be controlled by the relative amplitude excitation (distribution) between the elements of the array. In fact, there is a trade off between the beamwidth and the side lobe level based on the amplitude distribution of the elements [1]. In this issue, array technology is detailed in "Basic array theory," by W. H. Kummer, "Array pattern control and synthesis" by R. C. Hansen, "Antenna array architecture," by R. J. Mailloux, "Array technology," by R. Tang and R. W. Burns, and "Adaptive processing array systems," by W. F. Gabriel.

VIII. Asymptotic Methods

There is a plethora of antenna elements, many of which exhibit intricate configurations. To analyze each as a boundary value problem and obtain solutions in closed form, the antenna structure must be described by an orthogonal curvilinear coordinate system. This places severe restrictions on the type and number of antenna systems that can be analyzed using such a procedure. Therefore, other exact or approximate methods are often pursued. Two methods which in the last three decades have been preeminent in the analysis of many previously intractable antenna problems are the *Integral Equation* (IE) method [1], [18], [28], [33], [49]–[55], and the *Geometrical Theory of Diffraction* (GTD) [1], [18], [29], [33], [52], [56]–[61]. Numerical techniques have played a key role in their success. For structures that are not convenient to analyze by either of the two methods, a combination of the two is often used. Such a technique is referred to as a *hybrid method*, and it is described in more detail in "Overview of selected hybrid methods in radiating system analysis," by G. A. Thiele also in this issue. Most of the research in advancing and applying these methods to antennas and scatterers was started in the late 1950's and early 1960's.

Another method which is beginning to gain momentum in its application to antenna problems is the finite-difference time-domain method [62]. This method has been extensively used to analyze penetration and scattering problems [63], but it is now finding application to antenna radiation problems [64]–[66].

A. Integral Equation (IE) Method

This method casts the solution to the antenna problem in the form of an integral (hence its name) where the unknown, usually the induced current density, is part of the integrand. Numerical techniques such as the *MM* [1], [18], [29], [33], [49]–[54] are then used to solve for the unknown. Once the current density is found, the radiation integrals of Section III can be used to find the fields radiated and other system parameters. This method is most convenient for wire type antennas and more efficient for structures which are small electrically. One of the first objectives of this method is to formulate the IE for the problem at hand. In general, there are two types of IE's. One is referred to as the *Electric Field Integral Equation* (EFIE), and it is based on the boundary condition of the total tangential electric field. The other is the *Magnetic Field Integral Equation* (MFIE), and it is based on the boundary condition that expresses the total electric current density induced on the surface in terms of the incident magnetic field. The MFIE is only valid for closed surfaces. For some problems, it is more convenient to formulate an EFIE while for others it is more appropriate to use an MFIE. Advances, applications, and numerical issues of these methods are addressed in this issue in "Low-frequency computational electromagnetics for antenna analysis," by E. K. Miller and G. J. Burke.

B. Diffraction Methods

When the dimensions of the radiating system are many wavelengths, low-frequency methods are not as computationally efficient. However, high-frequency asymptotic techniques can be used to analyze many problems that are otherwise mathematically intractable. One such method that has received considerable attention and application over the years is the *GTD* [1], [18], [29], [33], [52], [55]–[60]. GTD is an extension of geometrical optics (GO), and it overcomes some of the limitations of GO by introducing a diffraction mechanism.

At high frequencies diffraction, like reflection and refraction, is a local phenomenon and it depends on two things:

1) the geometry of the object at the point of diffraction (edge, vertex, curved surface);
2) the amplitude, phase, and polarization of the incident field at the point of diffraction.

A field is associated with each diffracted ray, and the total field at a point is the sum of all the rays that pass through that point. Some of the diffracted rays enter the shadow regions and account for the field intensity there. The diffracted field, which is determined by a generalization of *Fermat's principle* [56], [57], is initiated at points on the surface of the object which create a discontinuity in the incident GO field (incident and reflected shadow boundaries). The theory, advances, and applications of GTD are addressed in this issue in "High-frequency techniques for antenna analysis," by P. H. Pathak.

IX. Conclusions

Antenna engineering has enjoyed a very successful period during the past four decades. Responsible for its success have been the introduction and technological advances of some new elements of radiation, such as aperture antennas, reflectors, frequency independent antennas, and microstrip antennas. Excitement has been created by the advancement of the low-frequency and high-frequency asymptotic methods which have been instrumental in analyzing many previously intractable problems. A major factor in the success of antenna technology has been the advances in computer architecture and numerical computation methods. Today antenna engineering is considered a truly fine engineering art.

Although a certain level of maturity has been attained, there are many challenging opportunities and problems to be solved. Phased array architecture integrating monolithic MIC technology is still a most challenging problem. Integration of new materials into antenna technology offers many opportunities, and asymptotic methods will play key roles in their incorporation and system performance. Computational electromagnetics using supercomputing capabilities will model complex electromagnetic wave interactions, in both the frequency and time domains. Innovative antenna designs to perform complex and demanding system functions always remain a challenge. New basic elements are always welcomed and offer refreshing opportunities.

Acknowledgment

The author would like to thank his two colleagues, J. T. Aberle and D. Cochran, for reviewing the manuscript, J. P. Gilb and K. Liu for the figures and three-dimensional plots, and Kathy Muckenhirn for the preparation of the manuscript.

References

[1] C. A. Balanis, *Antenna Theory: Analysis and Design.* New York: Wiley, 1982.
[2] J. D. Kraus, "Antennas since Hertz and Marconi," *IEEE Trans. Antennas Propagat.*, vol. AP-33, pp. 131–137, Feb. 1985.
[3] J. C. Maxwell, *A Treatise on Electricity and Magnetism.* London, U.K.: Oxford Univ. Press, 1873, 1904.

[4] S. Silver, Ed., *Microwave Antenna Theory and Design.* MIT Radiation Lab. Series, vol. 12. New York: McGraw-Hill, 1949.

[5] W. Stutzman, "Bibliography for antennas," *IEEE Antennas Propagat. Mag.*, vol. 32, pp. 54–57, Aug. 1990.

[6] J. Aharoni, *Antennae.* London, U.K.: Oxford Univ. Press, 1946.

[7] J. D. Kraus, *Antennas.* New York: McGraw-Hill, 1950 (first edition), 1988 (second edition).

[8] S. A. Schelkunoff, *Advanced Antenna Theory.* New York: Wiley, 1952.

[9] S. A. Schelkunoff and H. T. Friis, *Antenna Theory and Practice.* New York: Wiley, 1952.

[10] E. A. Laport, *Radio Antenna Engineering.* New York: McGraw-Hill, 1952.

[11] C. H. Walter, *Traveling Wave Antennas.* New York: McGraw-Hill, 1965.

[12] E. Wolff, *Antenna Analysis.* New York: Wiley, 1966 (first edition), Norwood, MA: Artech House, 1988 (second edition).

[13] L. V. Blake, *Antennas.* New York: Wiley, 1966 (first edition), Norwood, MA: Artech House, 1987 (second edition).

[14] W. L. Weeks, *Antenna Engineering.* New York: McGraw-Hill, 1968.

[15] E. Jordan and K. Balmain, *Electromagnetic Waves and Radiating Systems.* New York: Prentice-Hall, 1950 (first edition), 1968 (second edition).

[16] R. E. Collin and F. J. Zucker, Eds., *Antenna Theory*, pts. 1 and 2. New York: McGraw-Hill, 1969.

[17] W. V. T. Rusch and P. D. Potter, *Analysis of Reflector Antennas.* New York: Academic, 1970.

[18] W. L. Stutzman and G. A. Thiele, *Antenna Theory and Design.* New York: Wiley, 1981.

[19] R. S. Elliott, *Antenna Theory and Design.* New York: Prentice-Hall, 1981.

[20] K. F. Lee, *Principles of Antenna Theory.* New York: Wiley, 1984.

[21] R. E. Collin, *Antennas and Radiowave Propagation.* New York: McGraw-Hill, 1985.

[22] T. A. Milligan, *Modern Antenna Design.* New York: McGraw-Hill, 1985.

[23] J. R. Wait, *Introduction to Antennas and Propagation.* Hithin Herts, UK: IEE, 1986.

[24] F. R. Connor, *Antennas.* London: Edward Arnold, 1989.

[25] K. Chang (Ed.), *Handbook of Microwave and Optical Components.* New York: Wiley-Interscience, 1989, vol. I, chs. 10–13

[26] R. C. Johnson and H. Jasik, *Antenna Engineering Handbook.* New York: McGraw-Hill, 1961 (first edition), 1984 (second edition).

[27] R. C. Hansen, Ed., *Microwave Scanning Antennas, vol. I—Apertures; vol. II—Arrays, and vol. III—Frequency Scanning Arrays.* New York: Academic, 1964. (Reprinted, Los Altos, CA: Peninsula Publishing.)

[28] A. W. Rudge, K. Milne, A. D. Olver, and P. Knight, Eds., *The Handbook of Antenna Design*, vols. 1 and 2. London: Peter Peregrinus, 1982.

[29] Y. T. Lo and S. W. Lee, Eds., *Antenna Handbook: Theory, Applications, and Design.* New York: Van Nostrand Reinhold, 1988.

[30] I. J. Bahl and P. Bhartia, *Microstrip Antennas.* Norwood, MA: Artech House, 1980.

[31] J. R. James and P. S. Hall (Eds.), *Handbook of Microstrip Antennas*, vols. I and II. London: Peter Peregrinus, 1989.

[32] D. M. Pozar, *Antenna Design Using Personal Computers.* Norwood, MA: Artech House, 1985.

[33] C. A. Balanis, *Advanced Engineering Electromagnetics.* New York: Wiley, 1989.

[34] V. H. Rumsey, "Frequency independent antennas," in *1957 IRE Nat. Conv. Rec.*, pt. 1, pp. 114–118.

[35] J. D. Dyson, "The equiangular spiral antenna," *IRE Trans. Antennas Propagat.*, vol. AP-17, pp. 181–187, Apr. 1959.

[36] R. H. DuHamel and D. E. Isbell, "Broadband logarithmically periodic antenna structures," in *1957 IRE Nat. Conv. Rec.*, pt. 1, pp. 119–128.

[37] R. E. Munson, "Conformal microstrip antennas and mirostrip phased arrays," *IEEE Trans. Antennas Propagat.*, vol. AP-22, pp. 74–78, Jan. 1974.

[38] J. Q. Howell, "Microstrip antennas," *IEEE Trans. Antennas Propagat.*, vol. AP-23, pp. 90–93, Jan. 1975.

[39] A. G. Derneryd, "Linearly polarized microstrip antennas," *IEEE Trans. Antennas Propagat.*, vol. AP-24, pp. 846–851, Nov. 1976.

[40] L. C. Shen, S. A. Long, M. R. Allerding, and M. D. Walton, "Resonant frequency of a circular disc, printed-circuit antenna," *IEEE Trans. Antennas Propagat.*, vol. AP-25, pp. 595–596, July 1977.

[41] P. K. Agrawal and M. C. Bailey, "An analysis technique for microstrip antennas," *IEEE Trans. Antennas Propagat.*, vol. AP-25, pp. 756–759, Nov. 1977.

[42] Y. T. Lo, D. Solomon, and W. F. Richards, "Theory and experiment on microstrip antennas," *IEEE Trans. Antennas Propagat.*, vol. AP-27, pp. 137–145, Mar. 1979.

[43] N. K. Uzunoglu, N. G. Alexopoulos, and F. G. Fikioris, "Radiation properties of microstrip dipoles," *IEEE Trans. Antennas Propagat.*, vol. AP-27, pp. 853–858, Nov. 1979.

[44] K. R. Carver and J. W. Mink, "Microstrip antenna technology," *IEEE Trans. Antennas Propagat.*, vol. AP-29, pp. 2–24, Jan. 1981.

[45] E. K. Miller and J. A. Landt, "Direct time-domain techniques for transient radiation and scattering from wires," *Proc. IEEE*, vol. 68, pp. 1396–1423, Nov. 1980.

[46] "IEEE Standard Definitions of Terms for Antennas," IEEE Standard 145–1983, *IEEE Trans. Antenna Propagat.*, vol. AP-31, Part II of two parts, pp. 5–29, Nov. 1983.

[47] W. R. Scott, "A general program for plotting three-dimensional antenna patterns," *IEEE Antennas Propagat. Newsletter*, vol. 31, pp. 6–11, Dec. 1989.

[48] G. Sinclair, "The transmission and reflection of elliptically-polarized waves," *Proc. IRE*, vol. 38, pp. 148–151, Feb. 1950.

[49] E. Hallen, "Theoretical investigations into the transmitting and receiving qualities of antennae," *Nova Acta Regiae Soc. Sci. Upsaliensis*, Ser. IV, 11, no. 4, pp. 1–44, 1938.

[50] J. H. Richmond, "Digital computer solutions of the rigorous equations for scattering problems," *Proc. IEEE*, vol. 53, pp. 796–804, Aug. 1965.

[51] R. F. Harrington, "Matrix methods for field problems," *Proc. IEEE*, vol. 55, pp. 136–149, Feb. 1967.

[52] ——, *Field Computation by Moment Method.* New York: Macmillan, 1968.

[53] R. Mittra, Ed., *Computer Techniques for Electromagnetics.* Oxford, U.K.: Pergamon, 1973.

[54] R. Mittra, Ed., *Numerical and Asymptotic Techniques in Electromagnetics*, vol. 3. New York: Springer-Verlag, 1974.

[55] J. Moore and R. Pizer, Eds., *Moment Methods in Electromagnetics.* Letchworth, England: John Wiley Research Studies Press, 1984.

[56] J. B. Keller, "Diffraction by an aperture," *J. Appl. Phys.*, vol. 28, pp. 426–444, Apr. 1957.

[57] ——, "Geometrical theory of diffraction," *J. Opt. Soc. Amer.*, vol. 52, pp. 116–130, Feb. 1962.

[58] R. G. Kouyoumjian, "Asymptotic high-frequency methods," *Proc. IEEE*, vol. 53, pp. 864–876, Aug. 1965.

[59] P. H. Pathak and R. G. Kouyoumjian, "An analysis of the radiation from apertures on curved surfaces by the geometrical theory of diffraction," *Proc. IEEE*, vol. 62, pp. 1438–1447, Nov. 1974.

[60] R. G. Kouyoumjian and P. H. Pathak, "A uniform geometrical theory of diffraction for an edge in a perfectly conducting surface," *Proc. IEEE*, vol. 62, pp. 1448–1461, Nov. 1974.

[61] G. L. James, *Geometrical Theory of Diffraction for Electromagnetic Waves*, third ed. (revised). London, U.K.: Peregrinus, 1986.

[62] K. S. Yee, "Numerical solution of initial boundary value problems involving Maxwell's equations in isotropic media," *IEEE Trans. Antennas Propagat.*, vol. AP-14, pp. 302–307, May 1966.

[63] A. Taflove and K. R. Umashankar," Review of FD-TD numerical modeling of electromagnetic wave scattering and radar cross section," *Proc. IEEE*, vol. 77, pp. 682–699, May 1989.

[64] J. G. Maloney, G. S. Smith, and W. R. Scott, Jr., "Accurate computation of the radiation from simple antennas using the finite-difference time-domain method," *IEEE Trans. Antennas Propagat.*, vol. 38, pp. 1059–1068, July 1990.

[65] P. A. Tirkas and C. A. Balanis, "Finite-difference time-domain technique for antenna radiation," *1990 IEEE Antennas and Propagation Symp. Dig.*, vol. I, pp. 14–17, May 7–11, 1990.

[66] ——, "Finite-difference time-domain method for antenna radiation," *IEEE Trans. Antennas Propagat.*, vol. 40, Mar. 1992.

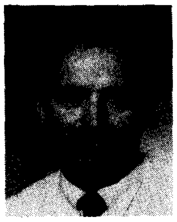

Constantine A. Balanis (Fellow, IEEE) was born in Trikala, Greece. He received the B.S.E.E. degree from Virginia Polytechnic Institute, Blacksburg, VA, in 1964, the M.E.E. degree from the University of Virginia, Charlottesville, VA, in 1966, and the Ph.D. degree in electrical engineering from Ohio State University, Columbus, OH, in 1969.

From 1964 to 1970 he was with NASA Langley Research Center, Hampton, VA. From 1970 to 1983 he was with the Department of Electrical Engineering, West Virginia University, Morgantown, WV. Since 1983 he has been at Arizona State University, Tempe, AZ, where he is presently Regents' Professor in the Department of Electrical Engineering and the Director of the Telecommunications Research Center. His research interests are in low- and high-frequency antenna and scattering methods, transient analysis and coupling of high-speed high-density integrated circuits, and multipath propagation.

Dr. Balanis is a member of ASEE, Sigma Xi, Electromagnetics Academy, Tau Beta Pi, Eta Kappa Nu, and Phi Kappa Phi. He served as Associate Editor of the IEEE TRANSACTIONS ON ANTENNAS AND PROPAGATION from 1974 to 1977 and of the IEEE TRANSACTIONS ON GEOSCIENCE AND REMOTE SENSING from 1982 to 1984. He served as Editor of the *Newsletter* for the IEEE Geoscience and Remote Sensing Society from 1982 to 1983 and as Second Vice-President of the IEEE Geoscience and Remote Sensing Society in 1984. He received the Graduate Teaching Excellence Award from the School of Engineering, Arizona State University for the 1987–1988 academic year. He is the author of *Antenna Theory: Analysis and Design* (Wiley, 1982) and *Advanced Engineering Electromagnetics* (Wiley, 1989).